Soft Matter

PAPER

View Article Online
View Journal | View Issue

Cite this: *Soft Matter*, 2017, **13**, 8250

Understanding chain folding morphology of semicrystalline polymers based on a rod–coil multiblock model

Faqiang Liu, Tongjie Sun, Ping Tang,* Hongdong Zhang and Feng Qiu

Received 20th September 2017,
Accepted 10th October 2017

DOI: 10.1039/c7sm01892d

rsc.li/soft-matter-journal

We employ a rod–coil multiblock molecular chain model to investigate chain folding behavior, which is a significant characteristic in semicrystalline polymers, by using the method of self-consistent field theory (SCFT). Polymer chains with different conformations in crystalline and amorphous regions are described by rigid rod chains and flexible Gaussian chains, respectively. At present, we concentrate on the thermodynamic behaviors of polymer semi-crystals after the formation of the initial lamellar crystals. A new mechanism for lamellar thickening is proposed to realize that the end of lamellar thickening depends on the crystallinity degree. In other words, it is impossible for lamellae to develop into extended-chain crystals by means of lamellar thickening if crystallinity is limited to a certain degree. We further discuss the competition between crystalline and amorphous regions and its influence on crystallization behaviors, such as the formation of double lamellae, chain tilt, the anomalies and adjacent re-entry. The synergistic influences of the driving force of crystallization, interfacial energy and crystallinity degree on chain folding behavior are also investigated when the density anomalies in amorphous regions are excluded. Our model demonstrates advantages in accurately describing the mesoscopic layered structures of semicrystalline polymers based upon a microscopic chain model and provides at least a semi-quantitative thermodynamic picture for chain folding.

1. Introduction

Polymer crystallization is a first-order transition between melts and extended-chain crystals (ECCs). Except for the crystallization immediately after polymerization[1,2] and the crystallization of low-molecular weight polymer melts,[3] polymer crystallization from melts starts with a nucleus formed by folding chains.[4] If particular conditions are satisfied to overcome the kinetic barrier, polymer chains will adjust their conformations from folding to straight to form a thermodynamic equilibrium state, *i.e.*, ECCs. Unfortunately, these conditions are rarely satisfied, and thus the phase transition is generally trapped in certain metastable states due to the complicated kinetic process of polymer crystallization. In this case, the metastable semi-crystal structures, such as spherulite and dendritic crystals, are formed instead of the thermodynamically stable ECC. Muthukumar[5] calculated the free energy landscape of a single chain and found that the lamella had a thickness much smaller than that of the extended chain. However, for the many-chain system, the ECC is generally considered as the equilibrium state.[6] In all of these metastable crystals, lamellae, *i.e.*, a semi-crystalline system containing alternating crystalline and amorphous layers, is the basic unit. Considering the huge mismatch between the long chain contour length and the lamellar thickness, chain folding in lamellae is inevitable,[7] which has also been proved by direct observations in experiments.[8,9] However, further understanding of the crystallization behaviors, such as lamellar thickening and chain folding, especially the underlying thermodynamic and kinetic mechanisms, is a longstanding difficulty.

Various experimental and theoretical investigations have been focused on chain folding behaviors in polymer crystals. Before the chain folding was experimentally observed at the atomic scale, various models had been put forward to describe the chain conformation in polymer crystals, such as the fringed micelle model,[10] folding chain model,[7] regularly folded model,[11,12] paracrystalline model,[13] switchboard model[14] and solidification model.[15] Discussions on the chain conformations of intra- and inter-lamellae are plentiful and it is now generally acknowledged that the chain details can be described by using different models according to different crystallization conditions. In other words, each proposed model is only suitable for the polymer crystals occurring in crystallization experiments at a specific kinetics process. For example, the microscopic structure formed by the crystallization of polymer melts at a high supercooling[16] is inclined to support the switchboard model, while the crystal

State Key Laboratory of Molecular Engineering of Polymers, Collaborative Innovation Center of Polymers and Polymer Composite Materials, Department of Macromolecular Science, Fudan University, Shanghai 200433, China.
E-mail: pingtang@fudan.edu.cn

structure crystallizing from dilute solution is suitably described by the regular folded chain model. However, there is no universal model that can explain all the crystalline issues in experiments.

Theoretical investigations were conducted to further interpret the experimental discoveries and probe the mechanisms of various thermodynamic and kinetic behaviors. The Lauritzen–Hoffman (LH) theory[12,17] investigated the relation between lamellar thickness corresponding to a maximum growth rate and temperature on the basis of thermodynamics, although they claimed the crystallization was a kinetics behavior. The Gibbs–Thomson (GT) equation[18] studied the relation between the temperature and minimum lamellar thickness. Further investigations based on molecular dynamics,[19] the Monte Carlo method,[20] the gambler ruin method[21] and lattice theory[22] indicated that the chain folding behavior was influenced by the folding energy, lamellar thickness, crystalline enthalpy and chain tilt.[23,24] In addition, the overcrowding in the amorphous region, the proportion of adjacent re-entry[23,25,26] and the kinetics of crystallization were discussed. Each model had a different emphasis in describing the diverse features of polymer chains in semicrystals. Flory's lattice model[22] and the gambler ruin method[21] concentrate on the amorphous regions. Most Monte Carlo investigations only focus on one lamella but ignore the interplay between the crystalline and amorphous regions. Since it was put forward, the widely used LH theory has become suspect because of some new experimental phenomena[5] and theories,[27] and the GT equation provides insufficient information on polymer crystallization behavior. In summary, the chain folding details, long chain characteristics and interplay between crystalline and amorphous regions are almost impossible to consider simultaneously in the theoretical models mentioned above. In experiments, the kinetic control in the preparation of samples and the single scale of most characterization methods limit a deep and systematic research on polymer crystallization. The difficulty and complexity involving polymer crystallization result from the chains' spanning from the microscale to the mesoscale. Therefore, a molecular level theory that can integrate the microscale of the stems in lamellae and the mesoscale of the whole chain trajectory is essential to describe the polymer chain in lamellar crystals.

It is well known that polymer chains entering the crystalline regions lose their conformation and turn stiff,[23,30–32] while the chains staying in the non-crystalline region closely match the bulk amorphous polymer[11,12] and possess the features of a Gaussian chain. Considering the profound conformation difference between the stiff and flexible chains,[33,34] it is essential to adopt different chain models to describe the chains in crystalline layers and in amorphous layers separately. Additionally, one polymer chain could cross several crystalline and amorphous layers due to its long chain character. Therefore, we propose a multiblock model to simulate the lamellar crystal of a semicrystalline polymer by the self-consistent field theory (SCFT), which has been extensively applied to investigate the microphase-separated structures of polymer systems. The molecular chain model containing multiple linked rods and coils is capable of simulating a polymer chain crossing crystalline and amorphous regions many times, as shown in Fig. 1. In this model, the chain stiffness in the crystalline region, the chain flexibility in the amorphous regions, the long-chain connectivity of polymers and the interaction between crystalline and amorphous layers are all considered at the same time. Our model shows advantages in understanding the chain folding behavior, which is the main characteristic in the condensed morphology of polymer crystals. For example, the chain tilt to the interface between the amorphous and crystalline regions is more easily investigated by our model, while this pronounced effect was generally ignored in other models.[7,23,35–38] By simulating the polymer chain in lamellae with rod–coil multi-blocks, we are able to explore the formation of different microstructures, such as double lamellae and a single lamella, and the chain folding details (chain tilt, adjacent re-entry) and their underlying thermodynamic mechanism, with the computational demand increased only slightly.

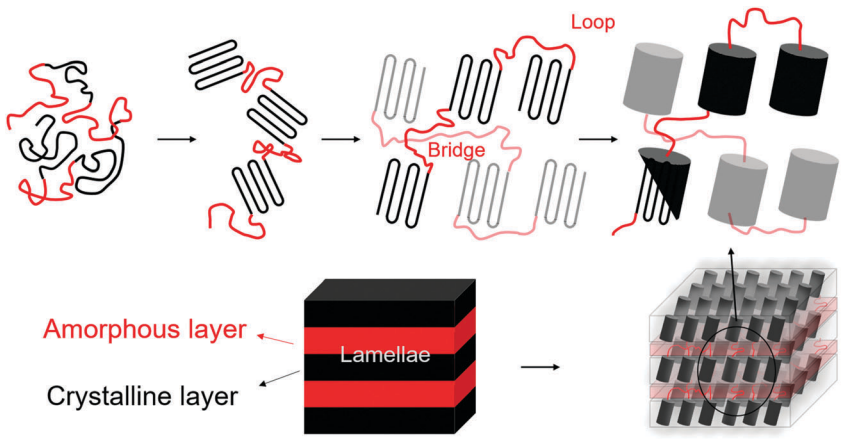

Fig. 1 Schematic representation of polymer chains with multi-blocks for simulation of the crystalline lamella structure. Upon crystallization, chains turn into a necklace-like structure in which the 'pearls' with rigid chains adopt an adjacent re-entry folding conformation, connected by flexible chains. Then the 'pearls' further align parallel to each other to form crystal lamellae, and amorphous and crystalline layers are arranged alternately in parallel. The schematic of the crystallization process agrees with various investigations.[5,28,29]

2. Theoretical model

SCFT has been extensively used to study polymer thermodynamic phase behavior at the mesoscale because of its high accuracy. It provides excellent theoretical support to the phase behaviors,[39,40] liquid crystal behaviors,[41–43] and mechanical properties[44] of inhomogeneous polymeric systems with various chain architectures. In the present work, SCFT is extended to rod–coil multi-block molecules in which the rod represents a bundle of crystalline stems and the coil represents the amorphous chain, as shown in Fig. 1. The SCFT theoretical framework for dealing with rod–coil multi-blocks is outlined as follows.

Consider an incompressible system with volume V containing n identical molecules; each molecule consists of rod and coil blocks representing the chain in crystalline and amorphous layers, respectively, as shown in Fig. 2. The flexible chains in the amorphous regions are modeled as Gaussian chains characterized by a statistical segment length a. The stiff chains in the crystalline layers are modeled as rigid rods characterized by a statistical length l and diameter d. For simplicity, the segments in the rod and coil chain are considered to have the same monomeric volume and thus the geometry dimension relations can be written as $a^3 = ld^2 = 1/\rho_0$, where $\rho_0 = nN/V$ (N is the total segment number per chain). The chain topology is represented by a sequence of n_R rods (R) and n_C coils (C). For example, RCRCR means a rod–coil–rod–coil–rod five-block molecule which contains three rods and two coils. The i-th rods and j-th coils have N_{R_i} and N_{C_j} segments, respectively. In the present work, all the rods have the same volume fraction, $f_{R_i} = f_r$, as do, for simplicity, the volume fractions of each coil. We adopt a parameter β to represent the geometrical asymmetry between the rods and coils in our calculation, which is written as follows:

$$\beta = \sqrt{6N}\frac{b}{a} \tag{1}$$

where b is the length of one rod segment and a is the statistical segment length of the coil chains; the monomeric volumes of the rod and coil chains are assumed to be the same, *i.e.* $\rho_0^{-1} = a^3 = bd^2$, where d is the diameter of rod. Here, a large value of β means a slim rod while a small one represents a short and stumpy rod. The volume fraction of all the rods represents the volume average crystallinity degree D, which is smaller than the weight average crystallinity as the chain in the crystalline region is generally denser than that in the amorphous region. The detailed derivation is similar to the SCFT for rod–coil diblock copolymers by Pryamitsyn and Ganesan[33] and has been described in our previous research.[45] The difference is that we adopt rod–coil multi-block molecules rather than diblock copolymers. In particular, the parameters in the SCFT are assigned new physical meaning to understand the chain folding in lamellae in the model of rod–coil multiblocks.

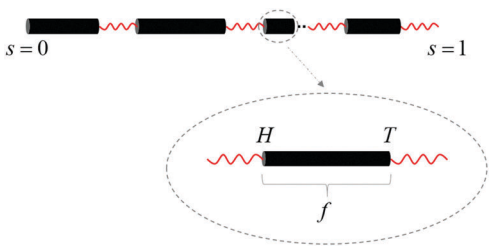

Fig. 2 Schematic illustration of rod–coil multiblocks for simulating the polymer chain crossing crystalline and amorphous regions many times. The chain is parameterized by a continuous variable s along the contour, the head and end of the chains are set to be $s = 0$ and $s = 1$. For an arbitrary rod in the molecule, as shown in the inset, $s = H$(head) and $s = T$(tail) represent the head and tail of the rod, respectively.

The main difference from a rod–coil diblock in the numerical algorithm is the calculation of the rod chain densities. For one rod in the polymer chain, as shown in the inset figure of Fig. 2, the distribution function of rods $q_R(\mathbf{r},\mathbf{u},s)$ represents the probability to find the s-th segment at position $\mathbf{r}$ with the orientation $\mathbf{u}$. It satisfies the modified diffusion equation:

$$q_R(\mathbf{r},\mathbf{u},s) = q_C(\mathbf{r}-\beta s\mathbf{u}, s=H)\exp\left\{-\int_0^s \mathrm{d}s'\Gamma(\mathbf{r}-\beta s'\mathbf{u},\mathbf{u})\right\} \tag{2}$$

Here, $\Gamma(\mathbf{r},\mathbf{u})$ is defined as

$$\Gamma(\mathbf{r},\mathbf{u}) = \omega_R(\mathbf{r}) - \mathbf{M}(\mathbf{r}) : \left(\mathbf{uu} - \frac{\mathbf{I}}{3}\right) \tag{3}$$

Where $\mathbf{I}$ is a 3×3 identical matrix. $\omega_R(\mathbf{r})$, $\omega_C(\mathbf{r})$ and $\mathbf{M}(\mathbf{r})$ represent the conjugated potential fields of the total densities of rods $\phi_R(\mathbf{r})$ and coils $\phi_C(\mathbf{r})$, and the orientation order parameter $\mathbf{T}(\mathbf{r})$, respectively. The distribution function of coil $q_C(\mathbf{r},s)$, described by the Gaussian chain model, satisfies the following modified diffusion equation:

$$\frac{\partial q_C(\mathbf{r},s)}{\partial s} = \left[R_g^2\nabla^2 - \omega_C(\mathbf{r})\right]q_C(\mathbf{r},s) \tag{4}$$

For rod–coil multi-blocks, the total chain propagator $q(\mathbf{r},s)$ is calculated from the beginning ($s = 0$) to the end ($s = 1$) and then recalculated $q^*(\mathbf{r},s)$ in an inverse direction to obtain the propagators of each junction point of each rod, $q(\mathbf{r},s = H/T)$ and $q^*(\mathbf{r},s = H/T)$. Then, for an arbitrary rod in the chain, we obtain its density:

$$\phi_R^i(\mathbf{r}) = q_C(\mathbf{r}-\beta s\mathbf{u}, s=H)q_R^*(\mathbf{r}+\beta\mathbf{u}(f_r-s), s=T) \times \exp\left\{-\int_0^{f_r}\mathrm{d}s'\Gamma(\mathbf{r}-\beta(s-s')\mathbf{u},\mathbf{u})\right\} \tag{5}$$

We adopt the Maier–Saupe interaction parameter γ to describe the orientational interaction between rods. The Flory–Huggins interaction parameter between rod and coil chains is represented by ε and the incompressibility of the system is ensured by $\eta(\mathbf{r})$. The spatial lengths of the system are scaled by $R_g = \alpha(N_C/6)^{1/2}$, the unperturbed radius of gyration of coil chain. The total free energy of a single chain is:

$$F = \frac{1}{V}\int \mathrm{d}\mathbf{r}\varepsilon\phi_C(\mathbf{r})\phi_R(\mathbf{r}) - \omega_C(\mathbf{r})\phi_C(\mathbf{r}) - \omega_R(\mathbf{r})\phi_R(\mathbf{r}) + \eta(\mathbf{r})(\phi_C(\mathbf{r})+\phi_R(\mathbf{r})-1) - \frac{\lambda}{2}\mathbf{T}(\mathbf{r}):\mathbf{T}(\mathbf{r}) + \mathbf{M}(\mathbf{r}):\mathbf{T}(\mathbf{r}) - \ln Q \tag{6}$$

where Q is partition function of a single chain

$$Q = \frac{1}{V}\int \mathrm{d}\mathbf{r} q(\mathbf{r}, s = 1) \tag{7}$$

The following SCFT equations are obtained by using a saddle point approximation to calculate the functional integrals of the partition function:

$$\omega_{\mathrm{c}}(\mathbf{r}) = \varepsilon\phi_{\mathrm{R}}(\mathbf{r}) + \eta(\mathbf{r}) \tag{8}$$

$$\omega_{\mathrm{R}}(\mathbf{r}) = \varepsilon\phi_{\mathrm{C}}(\mathbf{r}) + \eta(\mathbf{r}) \tag{9}$$

$$\phi_{\mathrm{C}}(\mathbf{r}) + \phi_{\mathrm{R}}(\mathbf{r}) = 1 \tag{10}$$

$$\phi_{\mathrm{C}}(\mathbf{r}) = \frac{1}{Q}\sum_{j=1}^{n_{\mathrm{C}}}\int_0^{f_{\mathrm{C}_j}} \mathrm{d}s q_{\mathrm{C}}(\mathbf{r}, s) q_{\mathrm{C}}{}^*(\mathbf{r}, s) \tag{11}$$

$$\phi_{\mathrm{R}}(\mathbf{r}) = \frac{1}{Q\int \mathrm{d}\mathbf{u}}\sum_{i=1}^{n_{\mathrm{R}}}\int_0^{1-f_{\mathrm{r}}} \mathrm{d}s q_{\mathrm{R}}(\mathbf{r} - \mathbf{u}\beta s, s = H) q_{\mathrm{R}}{}^*(\mathbf{r} + \mathbf{u}\beta(f_{\mathrm{r}} - s)) \times \exp\left\{-\int_0^{f_{\mathrm{r}}} \mathrm{d}s' \Gamma(\mathbf{r} - \mathbf{u}\beta(s - s'))\right\} \tag{12}$$

$$\mathbf{M}(\mathbf{r}) = \gamma\mathbf{T}(\mathbf{r}) \tag{13}$$

$$\mathbf{T}(\mathbf{r}) = \frac{1}{Q\int \mathrm{d}\mathbf{u}}\sum_{i=1}^{n_{\mathrm{R}}}\int_0^{1-f_{\mathrm{r}}} \mathrm{d}s q_{\mathrm{R}}(\mathbf{r} - \mathbf{u}\beta s, s = H) q_{\mathrm{R}}{}^*(\mathbf{r} + \mathbf{u}\beta(f_{\mathrm{r}} - s)) \times \exp\left\{-\int_0^{f_{\mathrm{r}}} \mathrm{d}s' \Gamma(\mathbf{r} - \mathbf{u}\beta(s - s'))\right\}\left(\mathbf{uu} - \frac{\mathbf{I}}{3}\right) \tag{14}$$

The SCFT equations can be solved numerically to obtain the chain details inside the lamellae, such as the chain folding and tilt. In order to obtain the relatively stable morphologies of the system, we start the calculation with specified various initial fields, and compare the calculated converged energies in different initial field, as well as with different lattice sizes. The final stable phase structure is thus determined as the one with the lowest free energy in the following calculations. The parameters mentioned above may possess different physical meanings for understanding the lamellar crystal morphology in the present work compared to the traditional rod–coil diblock, as discussed in what follows.

In the SCFT, two parameters ε and f are adopted to describe the phase behavior of coil–coil diblock copolymers. ε and f denote the Flory–Huggins interaction parameter between two different blocks and the volume fraction of one component, respectively. For rod–coil multi-blocks, two additional parameters are performed to characterize the rod chain, namely, the Maier–Saupe anisotropic orientation interaction parameter γ for the aligning of the rod chains and the geometrical asymmetry β between the rod and coil.[33] In our rod–coil multiblock model, these parameters are used to describe the behavior of the lamellar structure in polymer crystallization. When polymer chains enter into the crystals, several segments firstly turn straight at the expense of losing conformational entropy. On the other hand, the process that the straight segments creep into the crystalline region and release crystalline enthalpy contributes to reduce the free energy of the system, and thus compensates the entropic loss. Taking one lamella with lateral dimensions x, y and thickness L as an example, the surface energy associated with fold surfaces is σ_{e}, and the free energy change ΔF_{C} during crystallization can be expressed as follows:[17,23]

$$\Delta F_{\mathrm{C}}(T) = xyl(2\sigma_{\mathrm{e}}/L - \Delta H^{\infty}(T)\Delta T/T_{\mathrm{m}}) \tag{15}$$

where T_{m} and ΔH^{∞} are the equilibrium melting temperature and crystallization enthalpy of the perfect lamella with infinite size, and ΔT is the supercooling degree. In eqn (15), for the same polymer, the lower temperature corresponds to the larger supercooling and the larger free energy change during polymer crystallization. For different polymers at a particular temperature, the larger the crystallization enthalpy ΔH^{∞}, the larger the free energy change during crystallization. In our SCFT for the rod–coil multiblock model, the parameter γ, which is expected to depend inversely on the temperature[33] can simulate the driving force of crystallization. A large free energy change means a larger driving force in crystallization, corresponding to a larger γ in our model.

The parameter β represents the length–diameter ratio of the rods (the 'pearls' in Fig. 1), a large β means the length of the rod is large while the lateral size is small. β reflects the folding strategy for a part of the chain with a certain length; it may fold more times to form a short and stumpy rod or fold fewer times to form a long and thin rod, as shown in the inset of Fig. 3. For different polymers or different crystal structures of the same polymer, β also depends on the stacking density of the chains in the crystalline layer as stacking density varies with different polymer or different crystal structures. For example, the packing of the chains in a PE (polyethylene) crystal is tighter than that in a iPP (isotactic polypropylene) crystal (for α-iPP, the area per chain perpendicular to the chain axis is 0.45 nm^2 while it is 0.18 nm^2 for PE). So, for PE and iPP chains of same length with an identical number of folds, $\beta_{\mathrm{PE}} > \beta_{\mathrm{PP}}$. The stacking density also changes with the transformation of the crystal structure, such as an hexagonal PE and an orthorhombic PE.[46] Note that no chemical repulsion exists at the interface between the crystalline region and the amorphous region because the chemical species are the same. However, the segments adjacent to the interface between the crystalline and amorphous regions connect the rod and coil chain and lose their conformation, and yet no crystalline enthalpy is released because they have not folded into the crystalline region. The increase of the free energy resulting from the folding chain is considered as folding energy. Besides, the interface between crystalline and amorphous layers is generally rough, which also results in a free energy increase at the interface. As the folding energy and rough interface all happen at the interface between crystalline regions and amorphous regions, we propose an interface energy parameter ε to represent the surface energy, thus describing the combined effect of the folding energy and the surface roughness. Crystallinity degree is labeled as D, namely the total volume fraction of rods in the chains.

The SCFT based on a rod–coil multiblock chain model we adopted is extended to simulate semicrystalline polymers with a temperature dependent driving force as mentioned above. We note that our present method is a model for studying

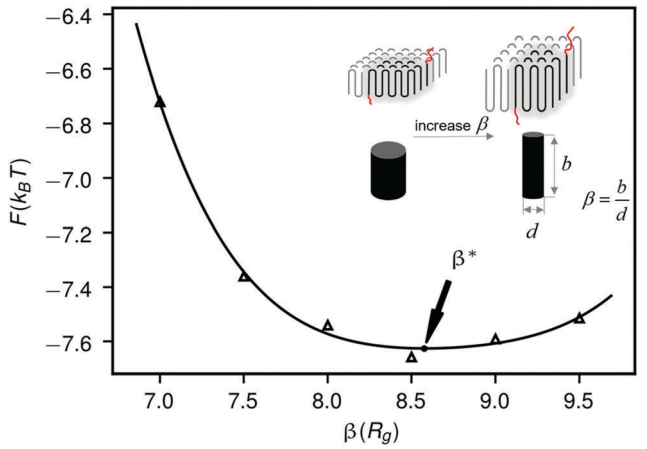

Fig. 3 Free energy F of a single chain as shown in eqn (6) plotted against length–diameter ratio β at ε = 40, γ = 200 and D = 0.5 for an RCRCR molecule. The inset is the schematic folding strategy difference between rods of different β. The part of the polymer chain with a fixed length that is destined to fold into the crystalline region and show an adjacent re-entry conformation may fold into a short and thick bundle, or a long and thin bundle, represented by rods with different length–diameter ratios β in our model. For the inset, the black straight lines represent the polymer chains in crystalline regions and the red curves represent the chains in amorphous regions.

polymer crystal morphology, similar to the work by Shah and Ganesan,[44] in which a semicrystalline copolymer is simulated by a semiflexible-flexible chain. With a decrease of temperature, the system exhibits only an isotropic–nematic transition, which is a liquid crystal behavior other than a crystallization behavior. In fact, it has been reported that the liquid crystal structure exists as an intermediate state before crystallization,[31] and thus the results obtained in our model are of valuable importance. In addition, we focus on the following thermodynamic information after the semicrystalline lamellar structure is formed, ignoring the early nucleation process. In this case, an accurate description of the chain conformations in the crystalline and amorphous regions is more important. As the chain segments are fixed in the crystal lattice, the stems in crystalline layers are fully rigid, which are represented by rigid rods in our model.

Considering the huge scale difference between the chain contour length and the lamellar thickness, a long polymer chain may cross crystalline and amorphous layers many times. To accurately describe the chain in lamellar crystals, a large number of rods and coils are essential in our model. However, it will be a time-consuming task to calculate so many blocks, and the detail of the chain trajectory in the lamellae will also be very difficult to trace with increasing number of the blocks. Considering the computation cost and the simulation precision comprehensively, we fix the block number to be 3–5 in the present work; the subsequent results prove the simplification is reasonable.

Our study aims to shed light on the chain folding behaviors and thus get a further understanding of the thermodynamic mechanism of various crystallization behaviors, such as lamellar thickness, lamellar thickening, and chain folding inter- and intra-lamellae. Although it is generally recognized that the lamellae structure is attributed to kinetics, driven by thermodynamics, the polymer chains tend to optimize their conformations inter- and intra-lamellae during and after the crystallization process. The thermodynamic driving adjustment of chain conformation is essential in polymer crystals, which will be discussed in the next section. In the SCFT for our rod–coil multi-block model, the folding behavior is driven by the interplay of the interface energy parameter ε, driving force parameter γ, length–diameter ratio β and crystallinity degree D. We note that these influencing parameters on the phase behavior are similar to those of rod–coil blocks. By fully characterizing the features of the polymer chain in lamellae, we are able to probe the folding behavior of polymer chains in polymer crystals and their corresponding thermodynamic mechanism.

3. Results and discussions

A chain may immediately go back to the crystalline layer it comes from, so the segments connecting the two stems do not enter the amorphous region, leading to the tight fold conformation, namely, adjacent re-entry. In addition, the chain may also go into the amorphous region, then a non-adjacent re-entry conformation, *i.e.*, loop (the stems connected by the loop belongs to the same crystalline layer) or bridge (the stems connected by the bridge belong to two adjacent crystalline layers) is formed. The three conformations have been extensively discussed in various models[11,12,24] and theories.[21,22] Among these models, the switchboard model[24] triggered a hot discussion in the 68th Faraday Discussion Meeting. This is due to the fact that the model involves a vital matter, namely, whether the adjacent re-entry is a rare event in the extensively intertwined chains in lamellae.[14,26,35,47] The results of the discussions indicate a high probability of the re-entry caused by the spatial packing effect, *i.e.*, a density anomaly or overcrowding happens if not enough space is provided in the amorphous regions. If all the stems in the crystalline layer emit the chains to the amorphous layer, the density of the amorphous layers will be much higher than that of the crystalline layers.[21,48] This is contrary to the fact that the density in the amorphous region is lower than that of the tight packing crystalline region. Moreover, apart from spatial packing factors, non-spatial packing factors, such as fold energy, lamellar thickness and crystalline enthalpy, may also have great effects on the chain folding behavior. In other words, we still need to address the situation that the bridge, loop and re-entry conformations mix together in polymer semi-crystals irrespective of the spatial packing effect in the amorphous regions. This problem has not been taken seriously in previous research as the most attention was focused on the spatial packing effect.[21] As an undiscriminating investigation of the spatial and non-spatial factors on the chain folding behavior may lead to confusion, we will carry out the discussion about the influence of the spatial and non-spatial effects separately.

3.1 Folding strategy and lamellar thickness

Polymer crystallization is a process that starts from nucleation under the control of kinetics, and finishes with the following

chain conformation adjustment[49] under the control of kinetics and thermodynamics. Lamellar thickening, mainly resulting from chain conformation adjustment, has long been tracked and studied. Herein, we try to figure out its underlying physical mechanism. Previous investigations[22,38] indicate that the lamellae must consist of a significant proportion of re-entry, otherwise overcrowding happens in the amorphous region. On average, the polymer chain will immediately fold back to the lamella it comes from several times before it goes into the amorphous layer. The chain in polymer crystal is described as a 'necklace', as shown in Fig. 1. The ratio between adjacent re-entry and polymer chains released to the amorphous region is described by the length–diameter ratio of the 'pearls' which is represented by β in our model. β indicates the folding strategies as shown in the inset of Fig. 3. For a part of the polymer chain with a certain length destined to fold into crystalline layer, a small β means the chain folding more times, indicating that more adjacent re-entry conformations were adopted before the chain goes back to the amorphous region. We calculate the system with different β values and obtain the free energy (F) landscape of β as shown in Fig. 3. To make the result more understandable, we calculate the corresponding lamellar thickness and turn the β–F figures to L–F figures, as shown in Fig. 4. The stem length in our system is calculated as

$$L_{\text{stem}} = \beta f_{\text{r}} \tag{16}$$

Considering the chain tilt, the lamellar thickness is:

$$L = \beta f_{\text{r}} \cos\theta \tag{17}$$

where f_{r} is the volume fraction of a single rod and θ is the tilt angle between the c axis (the direction of the chain stems) and the normal of the interface between the amorphous and crystalline regions. The results demonstrate that there exists a lamellar thickness L^* corresponding to the minimum energy, which also corresponds to an optimum folding strategy β^*. L^* is independent of the driving force parameter γ and interface energy parameter ε but increases with crystallinity D, which is reasonable considering eqn (17) and $D = 2f_{\text{r}}$ for the RCRC molecule. The free energy landscapes of lamella thickness L indicate that if the system reaches the thermodynamic metastable state at a fixed crystallinity degree D, the chains in the lamellae will adjust their folding strategy to L^*. Our calculation indicates a universal law of chain folding in semi-crystalline lamellae, that is, on average, a polymer chain needs to adopt certain number of adjacent re-entry conformations before it goes into the amorphous region. This makes the length–diameter ratio of the bundle of crystalline chains about β^* while the corresponding lamellar thickness is L^*.

The initial packing of polymer chains into the crystalline region highly depends on the kinetic factor, primarily the degree of supercooling. The driving force of crystallization is proportional to the degree of supercooling, as shown in eqn (15), and the kinetic activation energy increases with lamellar thickness increasing.[17,23] As the growth rate depends on the combined action of the kinetic activation energy and thermodynamic driving force, although a higher driving force is provided in the formation of thicker lamellae, thin lamellae dominate at the early stage of crystallization due to the low

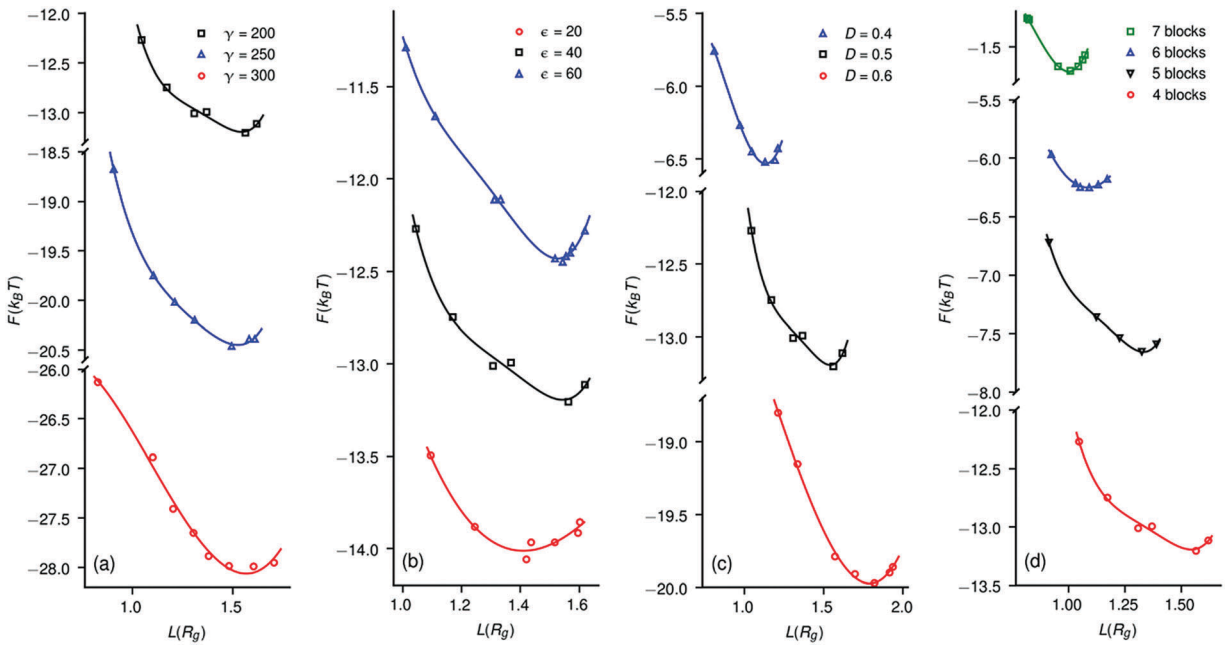

Fig. 4 Free energy F per chain as show in eqn (6) as a function of lamellar thickness L. (a) Different driving force parameter γ at $\varepsilon = 40$ and $D = 0.5$; (b) different interface energy parameter ε at $\gamma = 200$ and $D = 0.5$; (c) different crystallinity degree D at $\varepsilon = 40$ and $\gamma = 200$ for an RCRC of 4 blocks. (d) Different number of blocks in the molecule at $D = 0.5$, $\varepsilon = 40$ and $\gamma = 200$. 5, 6 and 7 blocks mean RCRCR, RCRCRC and RCRCRCR molecules, respectively. The same tendency of F as a function of L for molecules with a different number of blocks, as shown in (d), indicates our simplification that represents multiblock molecules with a certain number of blocks is reasonable.

activation energy. Yet the system with thin lamellae is not favored in thermodynamics because of the high free energy, as shown in Fig. 4. Driven by thermodynamics, the chain will adjust its conformation to reduce the free energy; as a consequence, L increases to L^*, namely the short, stumpy 'pearls' in Fig. 1 turn into slim and long ones, which is the typical adjustment of chain conformation during lamellar thickening.[50] As lamellar thickening happens when $L < L^*$ and the thickness of the initially formed lamellae L is always smaller than L^*, the crystallization temperature is generally below the melting temperature[51] because the initial lamellae is thinner than the final lamellae in the process of polymer crystallization. Besides, further thickening after L^* is impossible because of the absence of a driving force in the process from L^* to $L^* + \Delta L$ with a fixed D, that is, lamellar thickening ends at L^*. The results can also explain the fact that lamellar thickness for the common polymers, such as PE, PET, and PP, is about 10–50 nm[6,52–56] and it is hardly possible for lamella crystals to turn into the ECC by regular annealing. Previous studies suggest the higher kinetic barriers in lamellar thickening make the process slower and slower, and the thickening process seems endless in experiments. Yet, according to our result in Fig. 4, on the premise of the lamellar structure, polymer chains choose an appropriate folding strategy to form a bundle of chain segments with the length–diameter ratio β^*. The lamellar thickness reaches a certain value if crystallinity is fixed. The result is consistent with Flory,[22,57] who concluded that there is a suitable proportion between the adjacent re-entry and loop/bridge; the difference is that we yield the conclusion from the perspective of a larger scale and take many features of polymer chains in the lamellae into consideration.

The polymer chain will adopt a certain folding strategy β^* and obtain lamellar thickness L^* to reach the metastable state, as shown in Fig. 4. It is reasonable to speculate that if the arrangement of the chain in a crystalline layer is loose, to get the same β^*, a longer stem must be formed in loose-packing crystals due to the larger lateral size of the rod compared to the tight packing crystals. As we know, the α-phase iPP crystal is slightly denser than the β-phase one because the chain packing of the β-phase is more loose in the a and b axes than in the α-phase. Van der Meer[58] found that β-phase lamellae were much thicker than in the α-phase, with a slightly higher crystallinity degree, which proves our speculation.

With increasing crystallinity degree D, the free energy F significantly decreases (Fig. 4c) and the lamellar thickness increases, as described in eqn (16). In our opinion, lamellar thickness is limited by a limited crystallinity degree essentially resulting from the long chain property of polymers and the lack of chain mobility. For example, under a high temperature and pressure,[46] polyethylene crystal turns from orthorhombic to hexagonal, which greatly enhances the chain mobility and crystallinity degree, and then triggers a pronounced growth in lamellar thickness from the folding chain crystal to the extended-chain crystal. The results in Fig. 4 also demonstrate that the regularly folded model, which can be considered as the case at $\beta \to 0$, is not preferred for the polymer crystal emerging from the melt due to its high free energy. The same issue is unsuitable in our model for polymer crystals obtained from solution and the extended-chain crystals. For the extended-chain crystals, there are no amorphous regions and there is a huge difference between crystallization from a dilution solution and crystallization from a melt. Therefore, we note that the high crystallinity degree of a polymer crystal from a dilute solution is beyond the ability of our model. The same tendency of the free energy landscapes in Fig. 4d indicates that the number of blocks almost makes no difference in our calculations, which proves it is reasonable that we adopt a limited block approach to represent the polymer chain in polymer semi-crystals.

3.2 Double lamellae

Intriguingly, an unusual structure is found when β is relatively small. Different from traditional single lamellae in which one stem occupies the whole crystalline layer in the c axis, in the new structure, called double lamellae, the rod chains align head to head in one crystalline layer, as schematically shown in Fig. 5. Double lamellae are also found in experiments.[59,60] Whitmore and Noolandi[61] considered that the double lamellae were unstable because of the additional folds. Here, a new mechanism is proposed to explain the formation of double lamellae based on our model. It is known that the chain property results in a widely existing folding and entanglement in polymer crystals. To investigate polymer crystallization, the connection between several crystalline layers should be taken into consideration because of its significant influence on polymer crystals. Whitmore and Noolandi[61] considered only one lamella and concluded that the additional folds resulted in the increase of the free energy. In the present work, we make a different conclusion. On the one hand, the mechanism for the formation of the double lamellae is similar to the formation of the bilayer liquid crystal structure in our previous research.[34,60] Although the additional folds in the double lamellae increase the folding energy, the particular structure has half as many interfaces between the crystalline and amorphous regions compared with the interface in single lamellae, thus reducing the interface energy between the crystalline and amorphous regions. Therefore, the increased folding energy resulting from additional folds is compensated by the decrease of the interface energy. On the other hand, as mentioned above, rod chains with a small β are first formed at the early stage of polymer crystallization, and then the system tends to form double lamellae to reduce the surface between the amorphous and crystalline regions. If there is still enough surface for coil chains, the structure can be stabilized. In other words, the additional folds already exist before the formation of the double lamellae, so double lamellae may reduce the surface energy without adding additional folds to the system. Thus, we speculate double lamellae may also result from the first produced rod chains with a small β at the early stage of crystallization. Finally, the additional folds inside the double lamellae can also be compensated by other interactions. In Cheng's work,[59] the H-bonding at the end of short polymer chains enhanced the attraction between the separated layers of stems in one lamella. At the interface between the two layers in

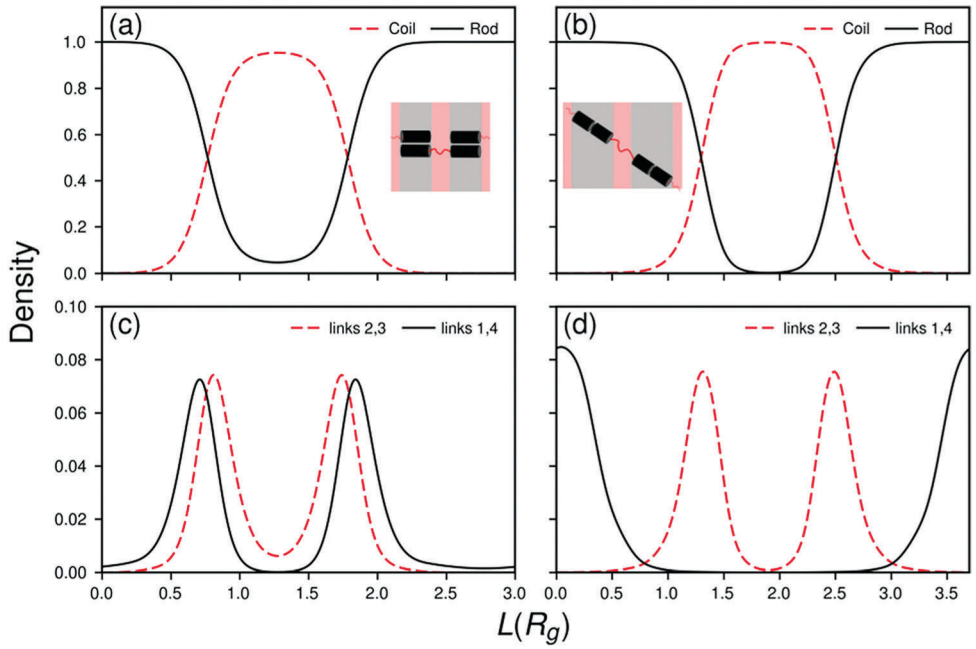

Fig. 5 Density profiles for (a) single lamellae with β = 6.2, (b) double lamellae with β = 6 for RCR molecules, ε = 20,γ = 100 and D = 0.67, (c and d) are the corresponding normalized density profiles of rod chain endpoints. In single and double lamellae, the rods assume an interdigitated arrangement and end-to-end arrangement, as shown in the insets of (a and b), respectively. The rods in (a) are perpendicular to the lamellae while in (b) the rods are inclined to the lamellae with a chain tilt angle θ of 50 degrees; θ is defined as the angle between the normal of the lamellae and the direction of the crystalline stems. In double lamellae, the chains adopt an adjacent re-entry conformation, *i.e.*, extremely tight fold[38] in the middle of crystalline layers where two crystalline stems meet, so overcrowding does not exist in these regions.

one lamella, the attraction of H-bonding may cancel out the increase of interface energy resulting from the additional folding. The research is consistent with our investigation that the interface energy between two layers of stems in one lamella is ignored.

As mentioned above, the double lamellae probably result from the initially produced rod chains with small β. In this case, we speculate that double lamellae may disappear with increasing β in the following lamellar thickening process. The ε *vs.* β phase diagram of an RCR molecule is calculated at γ = 100 and D = 0.67, as shown in Fig. 6a. The result indicates that with the increase of β, double lamellae turn to single lamellae. By comparing the free energy of candidate metastable structures, the one with the lowest energy is the stable phase. As shown in Fig. 6b, with the proper initial fields, the single (double) lamellae can be stabilized even in the double (single) lamellae phase region which is relatively far away from the phase boundary. This phenomenon is similar to the situation that polymer crystals are easily trapped in metastable states in the real crystallization process. The transition between double and single lamellae is reasonable considering the interface provided by the rod chains decreases with increasing β. The amorphous chains will be much stretched in double lamellae with the increase of β, thus favoring single lamellae formation. It is also noticed that with a larger interface energy parameter ε, the region of double lamellae in the phase diagram slightly increases. As the surface energy increases, the tendency for the system to reduce the surface energy becomes stronger, so double lamellae are stable at a large β with increasing surface energy. The phase diagram in Fig. 6a reveals that the double lamellae structure reduces the surface energy rather than increases the folding energy. The double lamellae structure can also be verified by a lamellar doubling process in the regularly stacked adjacent lamellae in the experiment by Rastogi *et al.*,[62] a novel way to thicken lamellae during the annealing of ultrahigh molecular weight polyethylene (M_w ~ 3000 kg mol^{-1}), which perfectly matches the process that double lamellae turn into single ones. We speculate that the existence of double lamellae is the reason why lamellar doubling could not happen again in the experiments by Rastogi *et al.* Up to now, double lamellae are only found in short chain systems. This phenomenon confirms our speculation that double lamellae are stabilized by a decreasing interface energy. For a short chain system, the entropy stretching loss is less important than the interfacial energy. With the increase of chain length, the stretching entropy becomes more important, and single lamellae are more stable because the structure provides more space for amorphous chains to release the conformation entropy.

3.3 Chain tilt and lamellar thickening

If β is too large, there is not enough space for amorphous chains so the system turns from double lamellae to single ones. To create more space for amorphous chains, the system tends to adopt new strategies such as adjacent re-entry conformations and chain tilts. As the arrangement of chains in a system with a

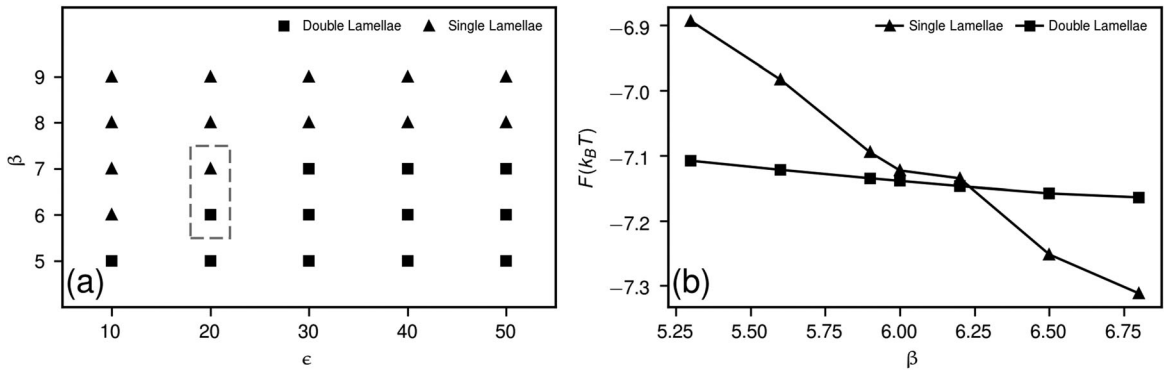

Fig. 6 (a) Phase diagram of RCR molecules in ε *versus* β, (b) free energy as a function of β in different phases at ε = 20, as shown in the dashed frame of (a) for the RCR molecule; other parameters are γ = 100 and D = 0.67. By adopting the initial field of single (double) lamellae, metastable single (double) lamellae can be stabilized, though the stable state is double (single) lamellae near the phase boundary.

large β is similar to the switchboard model, makes us pay attention to an old but important topic, density anomaly, *i.e.*, the overcrowding problem in amorphous regions. Previous investigations[21,22,38] mostly focused on the density anomaly at the interface between crystalline and amorphous layers and were confined to the microscale. Here we extend the density anomaly problem to the mesoscale in order to better understand the spatial requirement in amorphous regions. One should be aware that no overcrowding problem exists in a real system, because the density anomaly in amorphous regions, *i.e.*, chain overcrowding, means the polymer chains are compressed, yet the compression of solids or liquids will result in an increase of free energy several orders of magnitude larger than the effect of entropy and enthalpy. The density anomaly problem comes from inaccurate descriptions about the polymer chains in lamellae. The problem should be avoided in each model, otherwise the model does not make much sense. However, the reason why a density anomaly happens and how to avoid this problem are worth discussing, because this issue is responsible for many important crystallization behaviors, such as chain tilt, the ratio between adjacent re-entry and loop/bridge conformation.[38] If a particular kinetics is satisfied, lamellae that consist of rod chains with a larger β are formed, and there are three ways to release the density anomaly problem. Firstly, more chains in the amorphous regions creep into the crystalline region to reduce the volume fraction of the amorphous chains, as the density of the crystalline regions is generally higher than that of the amorphous regions, and thus more space is left for the remaining amorphous chains. Secondly, crystalline chains tilt to the interface, which has been proved to be an effective way to avoid the overcrowding problem.[38] And thirdly, if β is too large and the ways mentioned above are not effective enough, the crystalline lamellae develop a finite lateral width.[38] In other words, the bundles of crystalline chains disperse at the matrix of amorphous chains rather than forming a lamellar structure, the system may turn from a lamellar structure to other phases, such as the hexagonal cylinders in our previous investigation.[45] However, the kinetics may not allow the system to form such a well-defined structure. Though the way to reduce the density anomaly may also include the chain ends at the interface between the crystalline layers and amorphous layers,[38] the influence of chain ends is small for long chains and can be included in our parameter β, so the effect of chain ends on reducing the density anomaly is not listed alone in present work. Since the focus of our investigation is the thermodynamic properties of lamellae with a fixed crystallinity degree, only chain tilt is available to avoid the potential density anomaly problem.

If no chain tilt exists in the lamellae crystal, the interface area between the crystalline and amorphous regions decreases with the increase of β, so does the interface energy of the system. The amorphous chain at the interface will be much stretched, more importantly, a density anomaly happens. To release the overcrowding, the chain tends to tilt, which will result in an increase of the interface area at the same time.[6] If the surface energy per unit area is fixed (surface energy per unit area may vary with different tilt angles[63]), the increased interface leads to an increase of surface energy. The final tilt angle of the chain stems depends on the competition between the entropy loss of the amorphous chains and the interface energy. The length–diameter ratio β and the related tilt angle θ are plotted in Fig. 7. When $\beta > \beta^*$, the tilt angle increases with increasing β. The result also indicates that the chains in lamellae with different β more or less tilt to the interface between the crystalline and amorphous layers. This is consistent

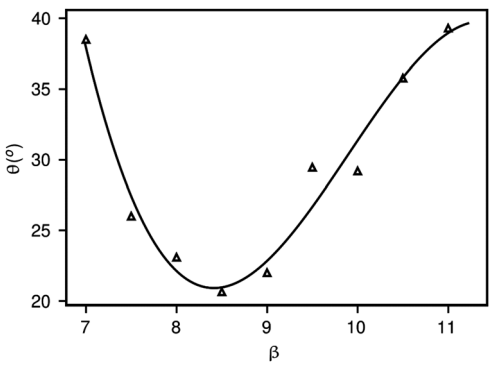

Fig. 7 The tilt angle θ plotted against the length–diameter ratio β at ε = 40, γ = 200 and D = 0.5 for an RCRCR molecule.

with the experimental fact that chain tilt is normal in polymer crystals while in polymer chains perpendicular to the folding surface it is a rare event.[38] Lamellae with β^* have the minimum tilt angle, and the chain tilt increases with increasing β. When β is larger than β^*, the free energy increases with increasing β as shown in Fig. 4. This reveals that chain tilt is not a panacea to deal with the overcrowding problem in amorphous regions, and stem tilt increases the interface energy by creating an excess interface, though it creates more space for amorphous regions. In lamellar crystals, the system can adjust the folding strategy and chain tilt to avoid the potential density anomaly and reach the final metastable state.

The traditional viewpoint suggests lamellae can thicken *via* the adjustment of chain conformation with chain sliding diffusion[50] or recrystallization. During chain sliding diffusion, the bundles of the chain exhibiting an adjacent re-entry conformation will adjust the conformation from short and stumpy bundles to thin and long bundles as shown in the inset of Fig. 3. Chain sliding diffusion requires a wide range of chain conformation adjustment, leading to a higher kinetic barrier. Herein, a new strategy to thicken lamellae is proposed, as shown in Fig. 8, namely, the adjustment of chain tilt. During the process of lamellar thickening, the length–diameter β increases while chain tilt is released at the same time, resulting in an increase of lamellae thickness L, as shown in eqn (17). The increase of lamellar thickness L is attributed to two processes, the increase of β *via* chain sliding diffusion and the decrease of θ *via* chain tilt adjustment, as shown in the inset of Fig. 8. Previous investigations ignore the chain tilt, so the thickening *via* chain tilt adjustment is also ignored. As chain tilt widely exists in polymer lamellae crystals,[38,64,65] lamellar thickening *via* chain tilt adjustment cannot be neglected. In our opinion, compared with the large kinetic barrier in chain sliding diffusion, lamellar thickening *via* chain sliding diffusion is not the preferred choice if chain tilt adjustment is available. In other words, if the stem in the lamellae inclines to the lamellae, the first choice to thicken the lamellae is to reduce the tilt. Of course, in the phenomenon that the stem in the lamellae is vertical to lamellae, only the first process is available.

In summary, a rod chain with a small β, namely, bundles of chain with a small size along the c axis and a large size in the a and b axes, emerge first, indicating that thin lamellae are formed first, as shown in Fig. 8. Yet the first formed thin lamellae are not favored in thermodynamics due to their high free energy, as shown in Fig. 4. Driven by thermodynamics, various crystallization behaviors arise, such as the formation of double lamellae, lamellar thickening and chain tilt. If enough chain mobility is provided and the crystallinity is fixed, the system will adopt the folding strategy corresponding to L^* (β^*) to reach a balance between the spatial requirement of amorphous chains and the interface energy. As long as L^* (β^*) is reached, no driving force exists for further thickening. In other words, lamellae cannot thicken anymore as long as L^* (β^*) is obtained, indicating that lamellae cannot turn into ECC *via* lamellar thickening. In our opinion, lamellar thickening has its limitation. The sustaining growth of the lamellar thickening in experiments is probably because the system has not reached β^*. The growing kinetic barrier in lamellar thickening slows down the rate of thickening, and if enough chain mobility is satisfied, the system will reach its favorite conformation, corresponding to β^*, and then lamellar thickening stops.

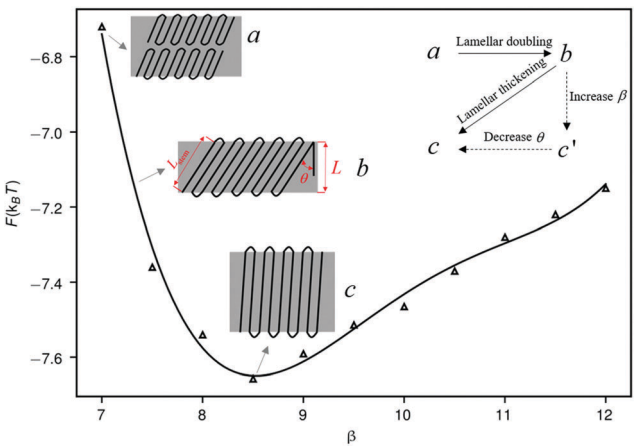

Fig. 8 Schematic representation of the thermodynamic driven crystallization behaviors after the initial formation of the lamellae. Firstly, if particular kinetic conditions are satisfied, double lamellae are formed. Then, during the following thickening process, double lamellae turn into single ones *via* lamellar doubling, a phenomenon in which the mutual chain rearrangement between two layers of stems in one lamella involves a sliding motion along the chain axis to double the stem length. Further thickening increases the length–diameter ratio β and decreases the tilt angle θ at the same time, as shown in Fig. 7. Two modes of chain movement in the lamellar thickening process are proposed in the upper right inset, namely, β increases from b to c′ *via* chain sliding diffusion and θ decreases from c′ to c *via* chain tilt adjustment.

3.4 Chain folding without consideration of the spatial effect

To date, tracing the trajectory of a long polymer chain inside the lamellae remains an important topic, both in experiment and in theory. Keller[7] firstly confirmed the chain folding in polymer crystals by comparing the contour length of a polymer chain and the lamellar thickness. Since then, a variety of detection methods have been used to trace chain trajectory, such as NMR,[66,67] neutron scattering (NS),[68] infrared (IR),[69] double quantum (DQ)[70] and AFM.[8,9] However, experimental investigations on chain folding are limited on the microscale or in short chains.[3,71] Furthermore, most experimental techniques are subject to special procedures or the particular morphology of the materials detected under harsh conditions, which further increases the difficulty in experiments. Previous theoretical investigations[22,24,35,37,38] on chain folding mainly focused on the ratio between adjacent re-entry and non-adjacent re-entry, which is related to the spatial packing effect. Yet for non-adjacent re-entry, *i.e.*, polymer chains go into amorphous regions rather than immediately back to the crystalline layers where they come from, two conformations are available, loop and bridge, as shown in Fig. 1. These two conformations were generally ignored in previous investigations, as the spatial effect seems much important and they are not fully understood yet. After the discussion of the spatial effect in the amorphous

region, we focus on the chain folding behavior without the distraction of the spatial effect. It is easy to be confused about the spatial effect and inter-lamellae chain folding behaviors. Our model is able to exclude the re-entry conformation and carry out a targeted investigation on inter-lamellae folding. By setting the length–diameter of the rod chains to be β^*, the chains in our system are regarded as that they have already adjusted their conformation to avoid overcrowding. In this case, the spatial packing effect is excluded.

In the SCFT calculation of the rod–coil system, the densities in the whole calculation space are equal to 1 due to the incompressible constraint. It is noted that the equal total density of the rod regions and coil regions does not violate the fact that the weight density of the crystalline region is greater than that of the amorphous region because the density here is the number density, not the generally considered volumetric mass density. The segments in the amorphous region and crystalline region have the same size but a different weight. Therefore, the equal maximum number densities of rods (crystalline chains) and coils (amorphous chains) does not contradict the different volumetric mass densities in the crystalline and amorphous regions. Previous research indicates that the interface is much thinner compared with the thickness of the crystalline or amorphous layer.[22,72] Herein, we adjust the driving force γ and interface energy ε to realize a relatively strong segregation to further accurately fit the real features of the polymer crystal in our system. Taking RCRCR 5-blocks as an example, the way to trace the specific chain trajectory is shown in Fig. 9. The initial lamellae structure is firstly calculated as the initial field, then the initial position of the molecule is fixed at a certain point on the edge of the crystalline layer (such as the black dot indicated in the top figure, let $\mathbf{r} = B$), which means:

$$q(\mathbf{r}, s = 0) = \begin{cases} 1, & \mathbf{r} = B \\ 0, & \mathbf{r} \neq B \end{cases} \quad (18)$$

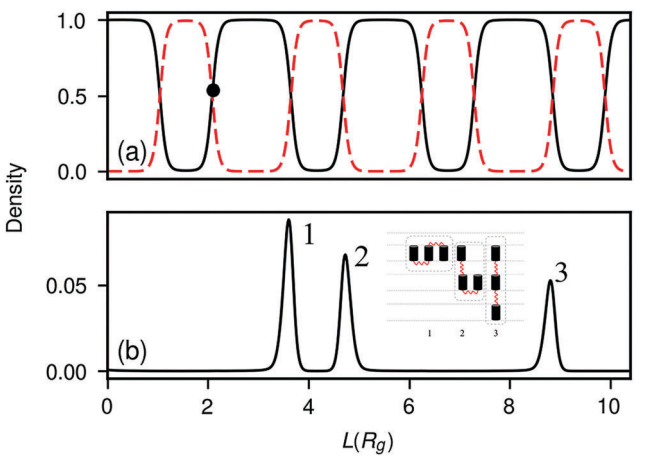

Fig. 9 The way to trace the trajectory of an RCRCR molecule. Density distributions of (a) rod $\phi_R(\mathbf{r})$ (black solid line) and coil $\phi_C(\mathbf{r})$(red dotted line), (b) chain end $\phi(\mathbf{r},s = 1)$ plotted as a function of L at $\varepsilon = 70$, $\gamma = 100$ and $\beta = 8$. The peaks 1, 2 and 3 in (b) correspond to the folding ways 1–3 in the inset, respectively.

Then the density distribution of the endpoint $\phi(\mathbf{r},s = 1)$ is calculated (the bottom figure). The peaks in different positions indicated different folding ways and the fraction of each folding way can be easily obtained by comparing the area of the peaks.

The movement after a chain exits a crystalline layer and goes into the amorphous layer is important due to its profound influence on the mechanical properties as well as a fundamental problem in polymer crystallization. A chain may fold back to form a loop conformation, or go forward to the next adjacent crystalline layer to form a bridge conformation. For a five-block molecule, there are three possible folding ways in the lamellae, as shown in the inset of Fig. 9b. As mentioned above, the probability of each folding way is possibly influenced by interface energy parameter ε, the driving force parameter γ, the length–diameter ratio β and the crystallinity degree D. The influence of γ on the probabilities of different conformations at different ε is calculated in Fig. 10, and the results indicate that the probability of conformation 1 decreases with γ increasing with a big ε, while conformation 3 shows the inverse trend. The influence of γ is not so obvious at small ε. The results indicate a synergistic effect of the interface energy and crystalline enthalpy on the chain folding. Hu and Tao[73] investigated the chain folding using Monte Carlo simulations and focused on the case of a tight re-entry conformation. They found that the fold-back conformation increased slightly with the temperature, a result consistent with our investigation. Note that our focus is on the folding behaviors of polymers chain in optimized metastable semi-crystals with different parameters. Thereby, we address our interest on the thermodynamic properties of the metastable lamellae, instead of the crystallization kinetics.

It is also observed that the probability of folding way 2 is roughly independent of the other parameters in Fig. 10a and b. Because folding way 2 combines bridge and loop conformations, as shown in the inset of Fig. 9, the influences of different parameters on these two conformations are cancelled out. Therefore, we adopt a limited number of blocks in the polymer molecule to represent the multiblock molecules, as a multiblock molecule with any number of blocks in our calculation only consists of two different kinds of conformation between two adjacent crystalline layers, that is, fold-back to form a loop or go forward to form a bridge. Thus, calculating more blocks just enhances the calculation difficulty to analyze the chain conformation and increases the computational cost, while the final results remain the same. Molecules that consist of different numbers of blocks are calculated and the result in Fig. 10d demonstrates that the influence of γ on chain folding shows the same tendency, suggesting our simplification is reasonable.

Since the spatial effect is included in the parameter β, no adjacent re-entry was taken into account here. However, one should keep in mind that the re-entry and loop conformation have no clear boundary in real system; the loop conformation may turn to re-entry if the chains in the amorphous region creep into the crystalline region.[74] Previous research did not define the clear boundary between loop and re-entry.[73] In our research, we averaged the length of the loop to reduce the computing complexity, and classified the adjacent re-entry into

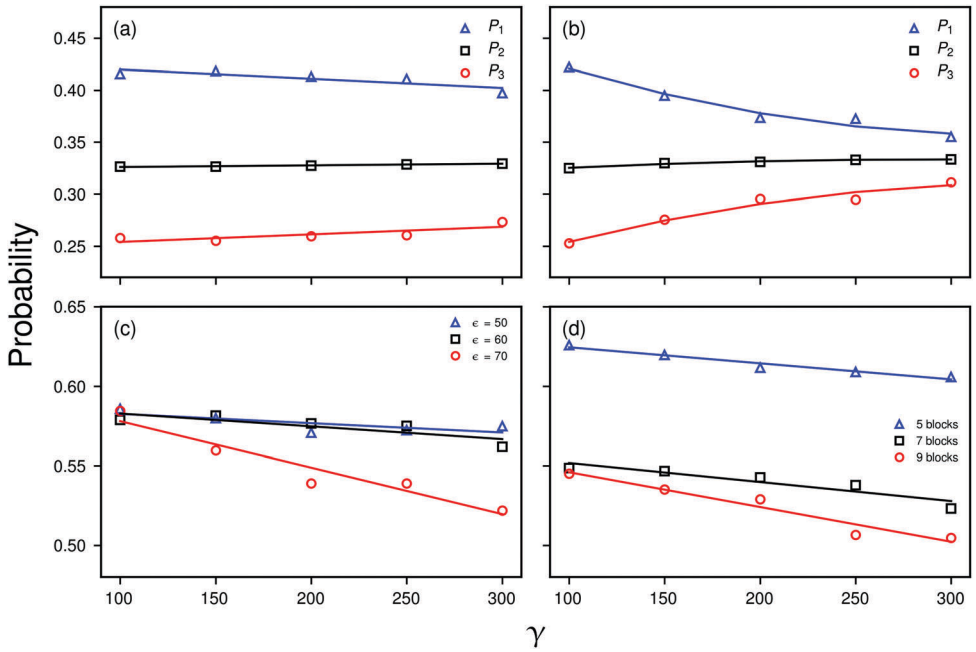

Fig. 10 γ influence on the probabilities of three folding ways at (a) ε = 60, and (b) ε = 70. (c) Probabilities of loop $P_L = P_1 + \frac{1}{2}P_2$ as a function of γ at different ε for RCRCR. Other parameters are β = 8 and D = 0.6. (d) Probabilities of loop conformation plotted as a function of γ for three different molecules, 5 block RCRCR, 7 block RCRCRCR, and 9 block RCRCRCRCR. The values of other parameters are ε = 50, D = 0.6 and β = 10.

parameter β, so the loop and re-entry can be distinguished. As shown in Fig. 10c, the proportion of the loop is higher than the bridge at small ε, but the proportion decreases with increasing ε. This observation demonstrates that the proportion of the chain fold back to the lamella it comes from is still large even without the consideration of space and geometry factors.

It is well known that lamellar thickening starts right after the polymer chains enter the crystalline region, and the lamellae thickness gradually increases during the isothermal crystallization process. The chain folding behavior may also change during the lamellar thickening process. Even though our investigations focus on the metastable state of the polymer crystal, the trend of the chain folding at different lamellae thickness L and different crystallinity D is still reasonable. The results in our calculation describe the condition that the lamellar thickening proceeds slowly, and thus the chains can fully adjust themselves before the thickness increase from L to $L + \Delta L$ and the crystallinity increases from D to $D + \Delta D$ within the time from t to $t + \Delta t$. Herein, the influence of β and crystallinity D on chain folding is shown in Fig. 11. The results indicate that the probability of the loop increases with β while decreases with D. During lamellar thickening, β increases *via* chain sliding diffusion and the crystalline degree D increases due to more chains creeping into the crystalline region. Because the influences of the two parameters (β, D) on P_L are opposite, we speculate that the probability of loop P_L may basically be unchanged in lamellar thickening, which needs to be proved in future investigations. It is noted that the infinitely long molecules in our model correspond to the system with long chains, since the contents of bridge/loop in the short chain system are much lower.[75,76]

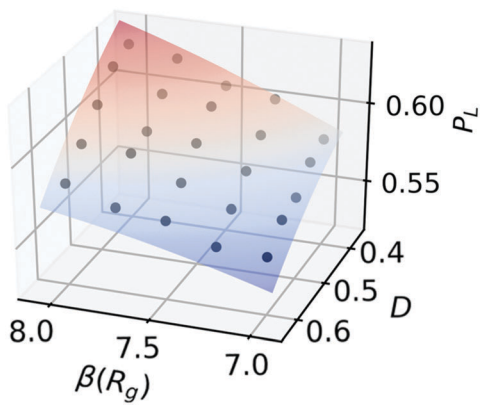

Fig. 11 Influence of β and D on the probability of loop P_L of a RCRCR polymer at ε = 40 and γ = 200. The black dots are the data points while the gray surface is the upward convex fitting surface.

4. Conclusions

In our present work, a rod–coil multi-block molecular model is adopted to simulate polymer chains in lamellae as a new viewpoint to investigate chain folding in semicrystalline polymers, using SCFT. Different conformations in the crystalline region and the amorphous region, chain connectivity, the tilt of chain in the crystalline region and the intra- and inter-lamellae interactions are taken into consideration in our system, which is difficult to realize in other models. A new description for polymer crystallization behavior is proposed in our work. Firstly, thin lamellae arise at an early stage under the control of kinetics.

Secondly, in the following process of chain conformation adjustment, various crystallization behaviors (lamellar thickening, formation of double lamellae and chain tilt) happen to reach a metastable state under the control of thermodynamics. Our investigation indicates that lamellar thickening finished when the folding strategy corresponds to the optimum L^* (β^*) with a fixed crystallinity. New mechanisms are proposed to explain various experimental phenomena, such as the formation of double lamellae and the fact that lamellae cannot turn into an extended-chain crystal *via* lamellar thickening. Finally, the kinetic barrier resulting from the limited chain mobility impedes the further increase of crystallinity and thus prevents further thickening of lamellae, and the chain conformation adjustment ends at this stage. Polymer crystallization is a process under kinetics–thermodynamics–kinetics control. The formation and disappearance of double lamellae structures are easy to understand if we take the whole crystallization process into consideration. We also prove that chain tilt is a common phenomenon which is consistent with experiments. Besides, the ratio between loop and bridge conformations, a vital chain folding behavior, is also investigated without the distraction of a spatial effect in the amorphous region. The factors that affect chain folding, such as the interface energy parameter ε, driving force of crystallization γ, crystallinity degree D and length–diameter ratio β are systematically investigated. The results show that the probability of loop P_L decreases with γ increasing and the decline is slower at a smaller ε, indicating a combined effect between γ and ε on P_L. P_L increases with increasing β and decreases with increasing D, which provides semiquantitative information on the chain conformation during lamellar thickening. Due to the great difficulty in fully describing the features of polymer chains in lamellae by other models, as an analogy, our model provides a new way to understand the various crystallization behaviors, such as lamellar thickening, the formation of double lamellae, chain tilt and so on.

Conflicts of interest

The authors declare no competing financial interest.

Acknowledgements

We thank financial support from the National Natural Science Foundation of China (Grant No. 21374023, 21574027 and 21320102005).

References

1 A. Keller, *Faraday Discuss. Chem. Soc.*, 1979, **68**, 145–166.
2 B. Wunderlich, *Angew. Chem., Int. Ed. Engl.*, 1968, **7**, 912–919.
3 S. Z. D. Cheng, A. Zhang, J. S. Barley, J. Chen, A. Habenschuss and P. R. Zschack, *Macromolecules*, 1991, **24**, 3937–3944.
4 B. Wunderlich and T. Davidson, *J. Polym. Sci., Part A-2*, 1969, **7**, 2043–2050.
5 M. Muthukumar, *Philos. Trans. R. Soc., A*, 2003, **361**, 539–556.
6 G. Reiter and G. R. Strobl, *Progress in understanding of polymer crystallization*, Springer, 2007.
7 A. Keller, *Philos. Mag.*, 1957, **2**, 1171–1175.
8 J. Kumaki, T. Kawauchi and E. Yashima, *J. Am. Chem. Soc.*, 2005, **127**, 5788–5789.
9 N. Mullin and J. K. Hobbs, *Phys. Rev. Lett.*, 2011, **107**, 197801.
10 W. Bryant, *J. Polym. Sci.*, 1947, **2**, 547–564.
11 A. Keller, *Rep. Prog. Phys.*, 1968, **31**, 623.
12 J. D. Hoffman and J. I. Lauritzen, *J. Res. Natl. Bur. Stand., Sect. A*, 1961, **65**, 297.
13 R. Hosemann, *J. Appl. Phys.*, 1963, **34**, 25–41.
14 D. Y. Yoon and P. J. Flory, *Polymer*, 1977, **18**, 509–513.
15 E. W. Fischer, *Pure Appl. Chem.*, 1978, **50**, 1319–1341.
16 J. Schelten, D. G. H. Ballard, G. D. Wignall, G. Longman and W. Schmatz, *Polymer*, 1976, **17**, 751–757.
17 J. Lauritzen and J. D. Hoffman, *J. Res. Natl. Bur. Stand., Sect. A*, 1960, **64**, 73–102.
18 B. Wunderlich and G. Czornyj, *Macromolecules*, 1977, **10**, 906–913.
19 T. A. Kavassalis and P. R. Sundararajan, *Macromolecules*, 1993, **26**, 4144–4150.
20 M. L. Mansfield, *Macromolecules*, 1983, **16**, 914–920.
21 C. M. Guttman, E. A. DiMarzio and J. D. Hoffman, *Polymer*, 1981, **22**, 1466–1479.
22 P. J. Flory, D. Y. Yoon and K. A. Dill, *Macromolecules*, 1984, **17**, 862–868.
23 J. D. Hoffman and R. L. Miller, *Polymer*, 1997, **38**, 3151–3212.
24 P. J. Flory, *J. Am. Chem. Soc.*, 1962, **84**, 2857–2867.
25 D. Yoon and P. Flory, *Macromolecules*, 1976, **9**, 294–299.
26 C. M. Guttman, J. D. Hoffman and E. A. DiMarzio, *Faraday Discuss. Chem. Soc.*, 1979, **68**, 297–309.
27 D. M. Sadler and G. H. Gilmer, *Phys. Rev. B: Condens. Matter Mater. Phys.*, 1988, **38**, 5684–5693.
28 T. Yamamoto, in *Interphases and Mesophases in Polymer Crystallization III*, ed. G. Allegra, Springer Berlin Heidelberg, Berlin, Heidelberg, 2005.
29 P. Welch and M. Muthukumar, *Phys. Rev. Lett.*, 2001, **87**, 218302.
30 P. D. Olmsted, W. C. K. Poon, T. C. B. McLeish, N. J. Terrill and A. J. Ryan, *Phys. Rev. Lett.*, 1998, **81**, 373–376.
31 G. Strobl, *Eur. Phys. J. E: Soft Matter Biol. Phys.*, 2000, **3**, 165–183.
32 B. Heck, S. Siegenführ, G. Strobl and R. Thomann, *Polymer*, 2007, **48**, 1352–1359.
33 V. Pryamitsyn and V. Ganesan, *J. Chem. Phys.*, 2004, **120**, 5824–5838.
34 W. Song, P. Tang, F. Qiu, Y. Yang and A. C. Shi, *J. Phys. Chem. B*, 2011, **115**, 8390–8400.
35 P. J. Flory and D. Y. Yoon, *Nature*, 1978, **272**, 226–229.
36 A. Peterlin, *Macromolecules*, 1980, **13**, 777–782.
37 D. Y. Yoon and P. J. Flory, *Macromolecules*, 1984, **17**, 868–871.
38 K. J. Fritzsching, K. Mao and K. Schmidt-Rohr, *Macromolecules*, 2017, **50**, 1521–1540.
39 K. K. Tenneti, X. Chen, C. Y. Li, Y. Tu, X. Wan, Q.-F. Zhou, I. Sics and B. S. Hsiao, *J. Am. Chem. Soc.*, 2005, **127**, 15481–15490.
40 L. Radzilowski, B. Carragher and S. I. Stupp, *Macromolecules*, 1997, **30**, 2110–2119.

41 B. D. Olsen, M. Shah, V. Ganesan and R. A. Segalman, *Macromolecules*, 2008, **41**, 6809–6817.
42 B. D. Olsen and R. A. Segalman, *Macromolecules*, 2007, **40**, 6922–6929.
43 Y.-d. Xia, J.-z. Chen, T.-f. Shi and L.-j. An, *Chin. J. Polym. Sci.*, 2013, **31**, 1242–1249.
44 M. Shah and V. Ganesan, *J. Chem. Phys.*, 2009, **130**, 054904.
45 J. Yu, F. Liu, P. Tang, F. Qiu, H. Zhang and Y. Yang, *Polymers*, 2016, **8**, 184.
46 S. Rastogi, L. Kurelec and P. J. Lemstra, *Macromolecules*, 1998, **31**, 5022–5031.
47 F. C. Frank, *Faraday Discuss. Chem. Soc.*, 1979, **68**, 7.
48 E. A. DiMarzio and C. M. Guttman, *Polymer*, 1980, **21**, 733–744.
49 J. Xu, Y. Ma, W. Hu, M. Rehahn and G. Reiter, *Nat. Mater.*, 2009, **8**, 348–353.
50 M. Hikosaka, K. Amano, S. Rastogi and A. Keller, *J. Mater. Sci.*, 2000, **35**, 5157–5168.
51 R. G. Alamo, B. D. Viers and L. Mandelkern, *Macromolecules*, 1995, **28**, 3205–3213.
52 F. A. Claudio De Rosa, *Crystals and Crystallinity in Polymers: Diffraction Analysis of Ordered and Disordered Crystals*, 2013.
53 H. Zhou and G. L. Wilkes, *Polymer*, 1997, **38**, 5735–5747.
54 J. J. Weeks, *J. Res. Natl. Bur. Stand., Sect. A*, 1963, **67**, 441.
55 A. Włochowicz and M. Eder, *Polymer*, 1984, **25**, 1268–1270.
56 E. Piorkowska and G. C. Rutledge, *Handbook of Polymer Crystallization*, 2013.
57 D. C. Bassett and A. M. Hodge, *Proc. R. Soc. A*, 1981, **377**, 25–37.
58 D. Van der Meer, *Structure-property relationships in isotactic polypropylene*, University of Twente, 2003.
59 S. Z. D. Cheng, H. S. Bu and B. Wunderlich, *Polymer*, 1988, **29**, 579–583.
60 A. Semenov and S. Vasilenko, *Sov. Phys. – JETP*, 1986, **90**, 124–140.
61 M. D. Whitmore and J. Noolandi, *Macromolecules*, 1988, **21**, 1482–1496.
62 S. Rastogi, A. B. Spoelstra, J. G. P. Goossens and P. J. Lemstra, *Macromolecules*, 1997, **30**, 7880–7889.
63 S. Gautam, S. Balijepalli and G. Rutledge, *Macromolecules*, 2000, **33**, 9136–9145.
64 M. Tasaki, H. Yamamoto, M. Hanesaka, K. Tashiro, E. Boz, K. B. Wagener, C. Ruiz-Orta and R. G. Alamo, *Macromolecules*, 2014, **47**, 4738–4749.
65 L. Mandelkern, *Acc. Chem. Res.*, 1990, **23**, 380–386.
66 X. Zeng, G. Ungar, S. J. Spells and S. M. King, *Macromolecules*, 2005, **38**, 7201–7204.
67 Y.-l. Hong and T. Miyoshi, *ACS Macro Lett.*, 2013, **2**, 501–505.
68 D. M. Sadler and A. Keller, *Science*, 1979, **203**, 263–265.
69 K. R. Reddy, K. Tashiro, T. Sakurai and N. Yamaguchi, *Macromolecules*, 2008, **41**, 9807–9813.
70 Y.-l. Hong, W. Chen, S. Yuan, J. Kang and T. Miyoshi, *ACS Macro Lett.*, 2016, **5**, 355–358.
71 S. Z. D. Cheng, J. Chen, A. Zhang, J. S. Barley, A. Habenschuss and P. R. Zschack, *Polymer*, 1992, **33**, 1140–1149.
72 L. Mandelkern, R. Alamo and M. Kennedy, *Macromolecules*, 1990, **23**, 4721–4723.
73 W. Hu and T. Cai, *Macromolecules*, 2008, **41**, 2049–2061.
74 J. U. Sommer and G. Reiter, *Europhys. Lett.*, 2001, **56**, 755–761.
75 R. Seguela, *J. Polym. Sci., Part B: Polym. Phys.*, 2005, **43**, 1729–1748.
76 Y.-L. Huang and N. Brown, *J. Mater. Sci.*, 1988, **23**, 3648–3655.